ACADEMIC PRESS

Available online at www.sciencedirect.com

SCIENCE DIRECT

Journal of Sound and Vibration 268 (2003) 881–895

JOURNAL OF SOUND AND VIBRATION

www.elsevier.com/locate/jsvi

A stiffness equation transfer method for natural frequencies of structures

Huiyu Xue*

Department of Physics, Suzhou University, Suzhou, Jiangsu 215006, China

Received 19 April 2002; accepted 10 December 2002

Abstract

A stiffness equation transfer method is proposed for obtaining vibration frequencies of structures. This method is an extension of the finite element-transfer matrix (FE-TM) method. In the present method, the transfer of state vectors from left to right in the ordinary FE-TM method is changed into the transfer of stiffness equations of every section from left to right. This method reduces the propagation of round-off errors produced in the ordinary transfer matrix method. Furthermore, the drawback that the number of degrees of freedom on the left boundary must be the same as that on the right boundary in the ordinary FE-TM method, is now avoided. Besides, this method finds out the values of the frequency by Newton–Raphson iteration method, so no plotting of the value of the determinant versus assumed frequency is necessary. An IFETM—W program based on this method for use on an IBM PC586 microcomputer is developed. Finally, numerical examples are presented to demonstrate the accuracy as well as the potential of the proposed method for free vibration analysis of structures.

1. Introduction

In vibration analysis of structures, exact solutions for the natural frequencies are possible only for a limited set of simple structures and boundary conditions. Approximate numerical methods are therefore important for the analysis of more complex systems. In numerical vibration analysis of engineering structures, the microcomputer has been playing an increasingly important role in China. The most powerful and most widely used numerical method in structural analysis is the finite element (FE) method. The disadvantage of the FE method, however, is that for some systems large matrices are produced which require large computers to handle them. In order to

*Corresponding author. Tel.: 86-0512-62520671.
E-mail address: xuehuiyu@sina.com (H. Xue).

doi:10.1016/S0022-460X(02)01606-1

reduce the size of the matrices, some substructure techniques have been proposed which consist of keeping the important degrees of freedom and suppressing the less important ones. Which degrees of freedom in the substructure are to be retained depends on judgment and on the physical system. But, this approach may lead to considerable inaccuracy if some degrees of freedom are wrongly suppressed.

The combined finite element-transfer matrix (FE-TM) method was proposed for the first time by Dokanish for free plate vibration problems [1]. Since then, several authors have proposed refinements and extensions of this method [2–14]. This method has the advantage of reducing the stiffness matrix size to a much smaller one than that obtained with the FE method and has been successfully applied to various linear and non-linear structural problems, such as static structural analysis, natural frequencies of structure, transient and steady state vibration response of structure, and non-linear dynamic response of structure. However, it is pointed out that recursive multiplications of the transfer and point matrices in ordinary FE-TM method are main sources of round-off errors. Particularly, in calculating high resonant frequencies or the response of a long structure, the numerical instability appears and it leads to an unwanted solution. The technique of exchanging state vectors and the Riccati transformation of state vectors were, respectively, used for solving these problems [5–8, 11–15]. In addition, the derivation of the transfer matrix from the dynamic stiffness matrix $[G]_i$ for strip i requires the inversion of the sub-matrix $[G_{12}]_i$ [1–3, 5–9]. In a strict sense, the inversion is possible only if $[G_{12}]_i$ is a square matrix. But $[G_{12}]_i$ is a square matrix only if there are equal numbers of nodes on the right boundary and on the left boundary of strip i. Therefore, most of the previous formulations of the combined FE-TM method are only applicable to models which have the same number of nodes on all the substructure boundaries. In order to alleviate this restriction on the finite element model, Degen et al. proposed a new FE-TM method based on a mixed finite element formulation [4]. Bhutani and Loewy proposed a procedure for deriving a transfer matrix by adding the zero elements to the state vectors which allows different number of nodes on the right and on the left boundary [10]. However, in these methods, recursive multiplications of the transfer and the point matrices are still necessary. Even though various techniques for treating these problems were presented [4–8, 10–14], research on this problem are as yet insufficient.

The purpose of this paper is to present a stiffness equation transfer (SET) method to overcome simultaneously both these two disadvantages in the ordinary FE-TM method. In the present method, the transfer of state vectors from left to right in the FE-TM method is transformed into a transfer of general stiffness equations in every section from left to right. Therefore, the inverse matrix of sub-matrix $[G_{12}]_i$ of the FE-TM method becomes the inverse matrix of sub-matrix $[G_{11}]_i$ of the present method. It is well known that $[G_{11}]_i$ is always a square matrix whether the structures are rectangular or not. Since the numerical solution of a two-point boundary value problem in the ordinary FE-TM method has been converted into the numerical solution of an initial value problem, the propagation of round-off errors occurring in recursive multiplications of the transfer and point matrices is avoided.

In the present method, the transfer matrix of stiffness equations and its derivatives with respect to frequency are formulated for the right boundary. This transfer matrix relation is then used in the determination of natural frequencies via a Newton–Raphson iterative technique. The present proposed method gives a quadratic convergence to a natural frequency from the trial value on either side of the true natural frequency and hence allows a greater degree of error in the selection of the trial frequency.

2. A stiffness equation transfer (SET) method

Without losing generality, we consider the plate shown in Fig. 1. It is divided into n strips and each strip is subdivided into finite elements. The vertical sides dividing or bordering the strips are called sections. It is apparent that the right of section i is the left of strip i.

2.1. An ordinary finite element-transfer matrix (FE-TM) method

Let $\{U\}_i$ and $\{N\}_i$ be the free vibration displacement and force vectors of strip i, $\{U\}_i^R$ and $\{N\}_i^R$ be the right free vibration displacement and force vectors of section i, $\{U\}_{i+1}^L$ and $\{N\}_{i+1}^L$ be the left free vibration displacement and force vectors of section $i+1$, so that we have

$$\begin{aligned} \{U\}_i &= [\{U\}_i^R, \{U\}_{i+1}^L]^{\mathrm{T}}, \\ \{N\}_i &= [\{N\}_i^R, \{N\}_{i+1}^L]^{\mathrm{T}}. \end{aligned} \tag{1}$$

If ω is the natural frequency of free vibrations, the equilibrium equations for the nodes on strip i can be written as

$$([K]_i - \omega^2[M]_i)\{U\}_i = \{N\}_i, \tag{2}$$

where $[K]_i$ and $[M]_i$ are the final stiffness and mass matrix of strip i, respectively.

Substituting Eq. (1) into Eq. (2), the later can be written as

$$[G]_i \begin{bmatrix} \{U\}_i^R \\ \{U\}_{i+1}^L \end{bmatrix} = \begin{Bmatrix} \{N\}_i^R \\ \{N\}_{i+1}^L \end{Bmatrix}, \tag{3}$$

in which

$$[G]_i = [K]_i - \omega^2[M]_i. \tag{4}$$

Matrix $[G]_i$ is the dynamic stiffness matrix for the strip i and it may be partitioned into four sub-matrices and Eq. (3) may be rewritten as

$$\begin{bmatrix} [G_{11}] & [G_{12}] \\ [G_{21}] & [G_{22}] \end{bmatrix}_i \begin{Bmatrix} \{U\}_i^R \\ \{U\}_{i+1}^L \end{Bmatrix} = \begin{Bmatrix} \{N\}_i^R \\ \{N\}_{i+1}^L \end{Bmatrix}. \tag{5}$$

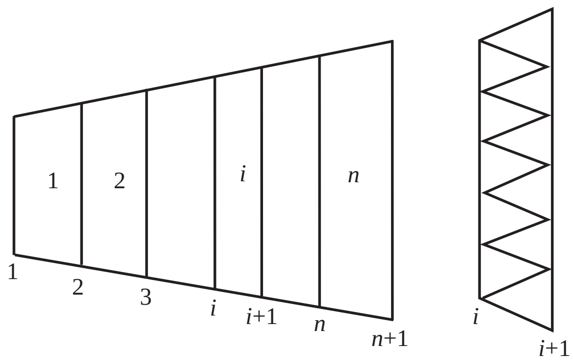

Fig. 1. Subdivision of structure into strips and finite elements.

The displacements are continuous across section i, so that we obtain

$$\{U\}_i^R = \{U\}_i^L. \tag{6}$$

Due to the continuity of force at section i, we obtain

$$\{N\}_i^R = -\{N\}_i^L. \tag{7}$$

Substituting Eq. (6) and Eq. (7) into Eq. (5), with a little algebraic manipulation, Eq. (5) can be rearranged to the form

$$\begin{Bmatrix} \{U\}_{i+1}^L \\ \{N\}_{i+1}^L \end{Bmatrix} = \begin{bmatrix} [T_{11}] & [T_{12}] \\ [T_{21}] & [T_{22}] \end{bmatrix}_i \begin{Bmatrix} \{U\}_i^L \\ \{N\}_i^L \end{Bmatrix} = [T]_i \begin{Bmatrix} \{U\}_i^L \\ \{N\}_i^L \end{Bmatrix}, \tag{8}$$

where

$$\begin{gathered} [T_{11}]_i = -[G_{12}]_i^{-1}[G_{11}]_i, \\ [T_{12}]_i = -[G_{12}]_i^{-1}, \\ [T_{21}]_i = [G_{21}]_i - [G_{22}]_i[G_{12}]_i^{-1}[G_{11}]_i, \\ [T_{22}]_i = -[G_{22}]_i[G_{12}]_i^{-1}. \end{gathered} \tag{9}$$

By proceeding in the same manner as in Ref. [1], we obtain the transfer matrix of the state vectors for the total structure:

$$\begin{Bmatrix} \{U\}_{n+1}^L \\ \{N\}_{n+1}^L \end{Bmatrix} = [P] \begin{Bmatrix} \{U\}_1^L \\ \{N\}_1^L \end{Bmatrix}, \tag{10}$$

in which

$$[P] = [T]_n[T]_{n-1} \cdots [T]_1. \tag{11}$$

Eq. (10) relates the section variables of the left boundary of the structure to those of the right boundary of the structure. The boundary conditions of the left edge of the structure would require some components of the state vectors to be zeros. Similarly, the boundary conditions of the right edge of the structure would also require certain components of the state vectors to be zeros. When these conditions are incorporated, it becomes essential that the determinant of a portion $[Q]$ of the matrix $[P]$ be zero at the correct natural frequency, for a non-trivial solution. That is, the natural frequencies are determined from the roots of the polynomial $\det[Q(\omega)] = 0$. In this method, it is obvious that the sub-matrix $[G_{12}]_i$ must be a square matrix in order to obtain $[T]_i$. In addition to this, propagation of round-off errors due to recursive multiplications of transfer matrix $[T]_i$ in Eq. (11) occurs.

2.2. Transfer matrix for stiffness equations

In order to overcome the drawback in the ordinary FE-TM method, the present method makes a change of the transfer of state vectors from left to right in the ordinary FE-TM method to the transfer of stiffness equations of every section from left to right. At the same time, the recursive multiplications of the transfer matrix $[T]_i$ are avoided.

Similarly as in generalized Riccati transformation of state vectors [15], we assume that the generalized stiffness equations which relate the force vectors to the displacement vectors on the left of section i are given by

$$\{N\}_i^L = [S]_i\{U\}_i^L + \{E\}_i \quad (i \geqslant 2), \tag{12}$$

where $[S]_i$, is the coefficient matrix of the stiffness equation for section i, and $\{E\}_i$, the equivalent external force vectors on the section i.

Substituting Eqs. (6) and (7) into Eq. (12), we obtain

$$\{N\}_i^R = -[S]_i\{U\}_i^R - \{E\}_i. \tag{13}$$

Eq. (13) describes the relation between the free vibration internal force vectors and the displacement vectors on the right of section i.

By expanding Eq. (5) and using a series of additional operations, we obtain

$$\{U\}_i^R = -[V]_i^{-1}[G_{12}]_i\{U\}_{i+1}^L - [V]_i^{-1}\{E\}_i, \tag{14}$$

and

$$\{N\}_{i+1}^L = [S]_{i+1}\{U\}_{i+1}^L + \{E\}_{i+1}, \tag{15}$$

where

$$[V]_i = [G_{11}]_i + [S]_i, \tag{16}$$

$$[S]_{i+1} = [G_{22}]_i - [G_{21}]_i[V]_i^{-1}[G_{12}]_i, \tag{17}$$

$$\{E\}_{i+1} = -[G_{21}]_i[V]_i^{-1}\{E\}_i. \tag{18}$$

Eq. (15) represents the relationships between the internal force vectors and the displacement vectors on the left of section $i+1$.

2.3. Transfer of entire structure

Supposing $[S]_2$ and $\{E\}_2$ are known, using Eqs. (17) and (18), $[S]$ and $\{E\}$ are transferred from the left of the second section to the right of the total structure. Hence, we have

$$\{N\}_{n+1}^L = [S]_{n+1}\{U\}_{n+1}^L + \{E\}_{n+1}. \tag{19}$$

It is worth noting that the transfer matrix $[P]$ in Eq. (10) for the ordinary FE-TM method is replaced by the stiffness equation matrix $[S]_{n+1}$ in Eq. (19) for the SET method. The dimension of matrix $[S]_{n+1}$ is only half that of the matrix $[P]$. In the SET method, the number of storage requirements would be only about half of the FE-TM method. In addition, the stiffness equation matrix $[S]_{n+1}$ is obtained by recursively using Eqs. (17) and (18) , and not by recursive multiplications of transfer and point matrices, so the propagation of round-off errors occurring in recursive multiplications of transfer and point matrices is avoided.

2.4. The method of determining $[S]_2$ and $\{E\}_2$

For strip 1, by expanding Eq. (5), we have

$$[G_{11}]_1\{U\}_1^R + [G_{12}]_1\{U\}_2^L = \{N\}_1^R, \tag{20}$$

$$[G_{21}]_1\{U\}_1^R + [G_{22}]_1\{U\}_2^L = \{N\}_2^L. \tag{21}$$

It is obvious that $\{U\}_1^R$ and $\{N\}_1^R$ may be determined by using the left-hand boundary conditions of the total structure. Since the left-hand boundary conditions are homogeneous, in general, we may discuss the following three cases:

2.4.1. Zero displacement boundary condition

Let the displacement vector of the left boundary $\{U\}_1^R$ be $\{0\}$. By Eq. (21), we obtain

$$[S]_2 = [G_{22}]_1, \tag{22}$$

$$\{E\}_2 = \{0\}. \tag{23}$$

2.4.2. Zero force boundary condition

Let the force vector of the left boundary $\{N\}_1^R$ be $\{0\}$. Hence from Eq. (20) $\{U\}_1^R$ is obtained. Then, substituting $\{U\}_1^R$ into Eq. (21), we have

$$[S]_2 = [G_{22}]_1 - [G_{21}]_1[G_{11}]_1^{-1}[G_{12}]_1, \tag{24}$$

$$\{E\}_2 = \{0\}. \tag{25}$$

2.4.3. Mixture boundary condition

In mixture boundary condition, we suppose $\{U\}_1^R = [\{U'\}_1^R, \{U''\}_1^R]^{\mathrm{T}}$ and the corresponding $\{N\}_1^R = [\{N'\}_1^R, \{N''\}_1^R]^{\mathrm{T}}$, in which $\{U''\}_1^R = \{0\}$, $\{N'\}_1^R = \{0\}$ and the corresponding $\{N''\}_1^R$ and $\{U'\}_1^R$ are unknown. For strip 1, Eq. (5) is rearranged and repartitioned. So we have

$$\begin{bmatrix} [H_{11}] & [H_{12}] & [H_{13}] \\ [H_{21}] & [H_{22}] & [H_{23}] \\ [H_{31}] & [H_{32}] & [H_{33}] \end{bmatrix} \begin{Bmatrix} \{U'\}_1^R \\ \{U''\}_1^R \\ \{U\}_2^L \end{Bmatrix} = \begin{Bmatrix} \{N'\}_1^R \\ \{N''\}_1^R \\ \{N\}_2^L \end{Bmatrix}. \tag{26}$$

Expanding Eq. (26) and solving the relations between $\{N\}_2^L$ and $\{U\}_2^L$, we obtain

$$[S]_2 = [H_{33}] - [H_{31}][H_{11}]^{-1}[H_{13}], \tag{27}$$

$$\{E\}_2 = \{0\}. \tag{28}$$

2.5. Determination of natural frequencies

From above, for different kinds of left homogeneous boundary conditions, we have $\{E\}_2 = \{0\}$. Using Eqs. (17) and (18), $[S]$ and $\{E\}$ are transferred from left to right through all the structures. Hence we have

$$\{N\}_{n+1}^{L} = [S]_{n+1}\{U\}_{n+1}^{L}, \tag{29}$$

$$\{E\}_2 = \{E\}_3 = \cdots = \{E\}_{n+1} = \{0\}. \tag{30}$$

The boundary conditions of the right edge of the structure usually require some components of state variables to be zeros. When these conditions are added, it becomes essential that the determinant of a portion $[Q]$ of the matrix $[S]_{n+1}$be zero at the correct natural frequency, for a non-trivial solution. Without losing generality, let $\{N\}_{n+1}^{L} = [\{N_1\}_{n+1}^{L}, \{0\}]^{\mathrm{T}}, \{U\}_{n+1}^{L} = [\{0\}, \{U_2\}_{n+1}^{L}]^{\mathrm{T}}$, in which $\{N_1\}_{n+1}^{L}$ is a portion of the force vector $\{N\}_{n+1}^{L}$ corresponding to non-zero elements at the right boundary and $\{U_2\}_{n+1}^{L}$ is a portion of the displacement vector $\{U\}_{n+1}^{L}$ corresponding to non-zero elements at the right boundary. According to the right boundary condition, from Eq. (29) we have

$$\left\{\begin{matrix} \{N_1\} \\ \{0\} \end{matrix}\right\}_{n+1}^{L} = \begin{bmatrix} [S_{11}] & [S_{12}] \\ [S_{21}] & [S_{22}] \end{bmatrix}_{n+1} \left\{\begin{matrix} \{0\} \\ \{U_2\} \end{matrix}\right\}_{n+1}^{L}. \tag{31}$$

This can be split into the following two equations:

$$\{N_1\}_{n+1}^{L} = [S_{12}]_{n+1}\{U_2\}_{n+1}^{L}, \tag{32}$$

$$\{0\} = [S_{22}]_{n+1}\{U_2\}_{n+1}^{L}. \tag{33}$$

For the non-trivial solution of Eq. (33), it is essential that the determinant of matrix $[S_{22}]_{n+1}$ be zero at the correct natural frequency. The matrix $[Q]$ is therefore, in this particular case, the matrix $[S_{22}]_{n+1}$. That is, the natural frequencies are determined from the roots of the polynomial

$$\Delta(\omega) = \det[Q(\omega)] = 0. \tag{34}$$

In general, the matrix $[Q]$ is obtained from matrix $[S]_{n+1}$ by deleting the columns corresponding to zero elements of $\{U\}_{n+1}^{L}$ and deleting the rows corresponding to the non-zero elements of $\{N\}_{n+1}^{L}$.

Now as in the work by Feng et al. [11], we also adopt the Newton–Raphson iteration technique as follows: differentiating Eqs. (16) and (17) with respect to ω, respectively, we obtain

$$[\dot{V}]_i = [\dot{G}_{11}]_i + [\dot{S}]_i, \tag{35}$$

$$[\dot{S}]_{i+1} = [\dot{G}_{22}]_i - [\dot{G}_{21}]_i[V]_i^{-1}[G_{12}]_i - [G_{21}]_i[V]_i^{-1}[\dot{G}_{12}]_i - [G_{21}]_i[\dot{V}]_i^{-1}[G_{12}]_i, \tag{36}$$

where the dot represents the differentiation with respect to ω. With a little algebraic manipulation, we have

$$[\dot{V}]_i^{-1} = -[V]_i^{-1}[\dot{V}]_i[V]_i^{-1}. \tag{37}$$

Substitution of Eq. (37) in Eq. (36) leads to

$$[\dot{S}]_{i+1} = [\dot{G}_{22}]_i - [\dot{G}_{21}]_i[V]_i^{-1}[G_{12}]_i - [G_{21}]_i[V]_i^{-1}[\dot{G}_{12}]_i + [G_{21}]_i[V]_i^{-1}[\dot{V}]_i[V]_i^{-1}[G_{12}]_i. \tag{38}$$

For different kinds of left-hand boundary condition, differentiating Eqs. (22), (24) and (27) with respect to ω, respectively, we have

for zero displacement boundary

$$[\dot{S}]_2 = [\dot{G}_{22}]_1, \tag{39}$$

for zero force boundary

$$[\dot{S}]_2 = [\dot{G}_{22}]_1 - [\dot{G}_{21}][G_{11}]_1^{-1}[G_{12}]_1 - [G_{21}]_1[G_{11}]_1^{-1}[\dot{G}_{12}]_1 + [G_{21}]_1[G_{11}]_1^{-1}[\dot{G}_{11}]_1[G_{11}]_1^{-1}[G_{12}]_1, \tag{40}$$

for mixture boundary

$$[\dot{S}]_2 = [\dot{H}_{33}]_1 - [\dot{H}_{31}][H_{11}]^{-1}[H_{13}] - [H_{31}][H_{11}]^{-1}[\dot{H}_{13}] + [H_{31}][H_{11}]^{-1}[\dot{H}_{11}][H_{11}]^{-1}[H_{13}]. \tag{41}$$

With Eqs. (38)–(41), $[\dot{S}]$ are transferred from left to right through all the structures, we obtain $[\dot{S}]_{n+1}$, and the matrix $[\dot{Q}]$ as well.

The recurrence relation between the trial frequencies based on the Newton–Raphson method is

$$\omega_{new} = \omega_{trial} - \frac{\det[Q]}{(\det[Q_1] + \det[Q_2] + \cdots + \det[Q_p])}, \tag{42}$$

where p is the order of the matrix $[Q]$. In Eq. (42), the determinants are evaluated at $\omega = \omega_{trial}$ and the coefficients of the matrices $[Q]_1, [Q]_2, \ldots, [Q]_p$ are identical to those of matrix $[Q]$ except for the following coefficients which are related to the coefficients of matrix $[\dot{Q}]$:

$$\begin{gathered} Q_1(i,1) = \dot{Q}(i,1), Q_2(i,2) = \dot{Q}(i,2), \ldots, \\ Q_p(i,p) = \dot{Q}(i,p), \; i = 1,2,\ldots,p. \end{gathered} \tag{43}$$

Since $[Q], [Q_1], [Q_2], \ldots, [Q_p]$ are known, they can be directly used in Eq. (42) to calculate the natural frequencies systematically.

The number of steps for convergence when using this method depends on the closeness of the initial frequency to the true natural frequency. In the vicinity of a root, the convergence is quadratic. Since the Newton–Raphson iteration technique requires a derivative of the function at each step, the computation time is doubled per step. However, this increase in computation time per step is offset by fewer steps for the same final accuracy. An additional advantage of the Newton–Raphson method is that it is a single point method requiring only one initial trial value. Besides, it has a known sufficient condition for convergence [16] given by $|\omega_{trial} - \omega_{true}| \leqslant d/(n-1)$, where d is the separation between the true natural frequency under consideration and its nearest neighboring natural frequency, and n is the degree of the polynomial $\Delta(\omega)$ under consideration.

3. Numerical examples

In order to examine the accuracy and the computation efficiency of our method, we developed a program IFETM–W on an IBM PC586 microcomputer. In this section, a flat, cantilevered triangular plate is first analyzed to obtain its fundamental frequency for checking purposes, and then the natural frequencies of the simply supported plate and the shear-wall structure with supporting frames are given to illustrate the validity of the proposed method.

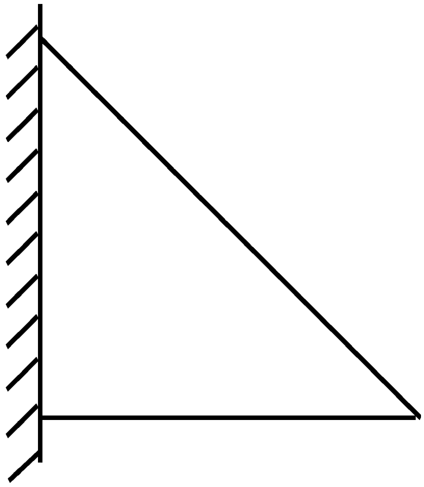

Fig. 2. A triangular cantilevered plate.

Table 1
Comparison of the SET method result with experiment result for the case of a flat triangular cantilevered plate

No. of segments/side	No. of elements	Fundamental frequency (Hz)
2	4	28.89
3	9	32.45
4	16	34.48
Experimental	—	34.5 [17]

The first example considered here is a flat, cantilevered, triangular plate shown in Fig. 2. The material and geometric properties are: Young's modulus $E = 2.07 \times 10^{11}$ Pa, mass density $\rho = 7850\,\mathrm{kg/m^3}$, the Poisson ratio $\mu = 0.3$, isosceles side length = 0.254 m, and plate thickness = 1.55×10^{-3}. The experimental value of the fundamental frequency given by Gustafson et al. is 34.5 Hz [17]. Bathe and his colleagues applied the standard finite element method based on the discrete Kirchhoff theory using a mesh with four segments per side [18]. The value of the first natural frequency obtained was also 34.5 Hz. For the present study, three cases with increasing number of substructures were studied. For the first case, the plate structure was modelled as one of two substructures; for the second case the structure was divided into three substructures and so on. Each substructure was further divided into triangular elements such that the plate has an equal number of segments per side. A three–node plate element was used to formulate the element elastic matrices for each substructure [19]. A lumped mass representation was used to form the mass matrix of the substructure. The mass of each substructure was assumed to be concentrated at the substructure interfaces only. The nodal mass m in the mass matrix was calculated as $m = \frac{1}{3}m_t$, where m_t is the total mass of all the triangular elements connected to that node. Table 1 shows agreement between the frequency calculated by the present SET method and the experimental result. The frequency increases initially when the number of substructures is increased and then converges to 34.5 Hz. In this example, the number of nodes on the left boundary is different from that on the right boundary. Most of the ordinary FE-TM method can only be applied to the

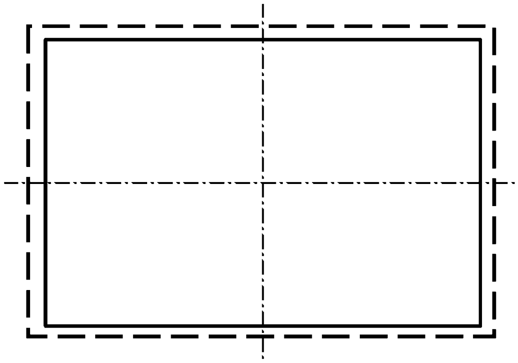

Fig. 3. Simply supported rectangular plate model.

Table 2
Comparison of natural frequencies for simply supported rectangular plate (Hz)

Mode numbers	FE	FE-TM	SET	Exact solution
1	5.317	5.318	5.318	5.329
2	10.20	10.19	10.19	10.25
3	16.33	16.34	16.33	16.40
4	18.31	18.31	18.31	18.45
5	21.09	21.02	21.09	21.31
6	29.05	28.90	29.08	29.52
7	29.36	29.20	29.33	29.92
8	34.04	33.63	33.99	34.85
9	38.74	38.20	38.76	39.74

chain-like structure which has equal number of degrees of freedom on the boundaries, so the ordinary FE-TM method and the combined finite element- Riccati transfer matrix (FE-RTM) method [1–3, 5–9] could not be used in this case. The present method has potentially wider application than the ordinary FE-TM method and the FE-RTM method.

The second example is to obtain the first nine natural frequencies of a simply supported rectangular plate as shown in Fig. 3. The plate chosen is 200 cm $\times$ 300 cm $\times$ 0.6 cm with a specific weight of 24.74 kN/m^3, $\mu = 0.23, E = 6.895 \times 10^4$ MPa. This problem has an exact analytical solution. We can compare the computed result with the exact solution. In the numerical calculation, the plate was divided into 30 strips and each of them subdivided into 40 triangular plate elements. The stiffness matrix and mass matrix of the plate element were formed in the same way as Example 1. Table 2 shows a comparison of natural frequencies among the exact analytical solution , SET solutions, FE solutions and the ordinary FE-TM solutions, where SET, FE and FE-TM methods are applied to the same mesh pattern. Table 3 shows the computation time for each method. Table 4 shows the comparison of the maximum mode displacements at the right boundary in our example (the maximum mode displacement at all nodes is normalized to 1). From the above results, it is found that SET method has the same accuracy of the FE method by using the same element mesh pattern, but higher computation efficiency. In comparison with the ordinary FE-TM method, it has lower round-off errors and higher computation efficiency.

Table 3
Comparison of computation time for simply supported rectangular plate

Method by applying	Computation time (s)
FE	310
FE-TM	228
SET	168

Table 4
The maximum mode displacement w at the right boundary of the simply supported rectangular plate (the maximum mode displacement w at all nodes is normalized to 1)

Mode numbers	SET	FE-TM
1	0.0	0.0017
2	0.0	0.0028
3	0.0	0.0154
4	0.0	0.0475
5	0.0	0.0852
6	0.0	0.1247
7	0.0	0.1343
8	0.0	0.1625
9	0.0	0.1891

Especially, the mode displacements at the right boundary in our example should be zero. However in the ordinary FE-TM method, owing to the propagation of round-off errors occurring in recursive multiplications of transfer and point matrices, they are not. This discrepancy becomes more serious for the higher modes. Our SET method can reduce the propagation of round-off errors produced in the ordinary FE-TM method.

In the third example, we analyzed a shear-wall structure with supporting frames to demonstrate the wider applicability of the present method. The present SET method not only be applied to the ordinary plate, but also to the other structures. Consider the shear-wall structure shown in Fig. 4, each node has six degrees of freedom:$u, v, w, \theta_x, \theta_y, \theta_z$. The shear-wall consists of 30 rectangular plate elements, where the physical and geometric parameters of each plate element are as follows: $E = 3 \times 10^{10}$ Pa, $\mu = 0.1667, \rho = 3000\,\mathrm{kg/m^3}$,thickness $t = 0.2$ m, length $l = 8$ m, and width $b = 3$ m. A four-node plane stress element was used to formulate the element elastic matrices [19]. A lumped mass representation was used to formulate the mass matrices. The total number of beam and column elements forming the supporting frames is 150. The physical and geometric parameters of them are as follows: $E = 3 \times 10^{12}$ Pa, $\rho = 2500\,\mathrm{kg/m^3}$. For horizontal beams, the dimension is $8\,\mathrm{m} \times 0.28\,\mathrm{m} \times 0.28\,\mathrm{m}$. For longitudinal columns, that is $3\,\mathrm{m} \times 0.4\,\mathrm{m} \times 0.4\,\mathrm{m}$. In addition, on the nodes 46, 48, 50, 52, 54, there are lumped mass of 5000 kg, respectively. Tables 5 and 6 show a comparison among the SET solutions, FE-TM solutions and the FE solutions. Table 7 shows the comparison of the maximum mode moments at the top boundary in our example (the maximum mode moment at all nodes is normalized to 1). Similar results as in Example 2 are obtained. It is worth noticing that the mode moments at the top boundary in our

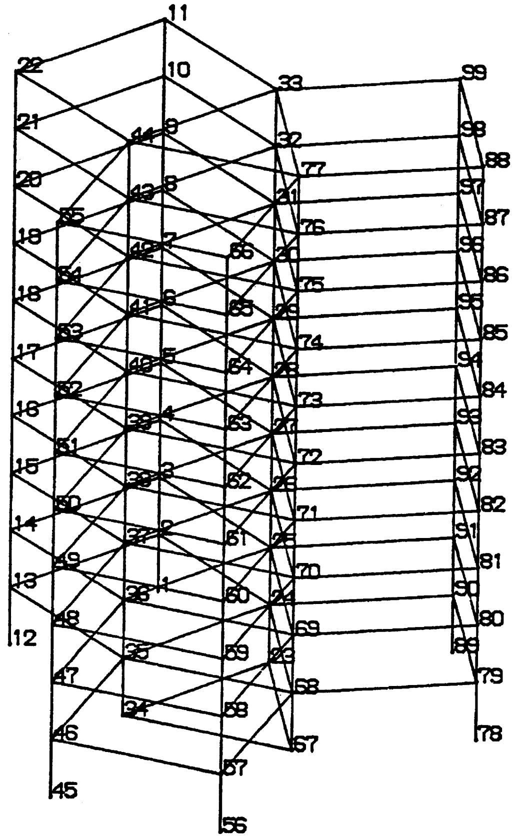

Fig. 4. A shear-wall structure.

Table 5
Comparison of natural frequencies of the shear-wall structure (Hz)

Mode number	FE	FE-TM	SET
1	3.194	3.192	3.193
2	3.248	3.254	3.251
3	4.069	4.079	4.074
4	10.83	10.69	10.78
5	11.92	11.79	12.03
6	14.76	14.58	14.69
7	15.02	14.86	14.91
8	16.66	16.48	16.60
9	17.01	16.82	16.95

example should be zero. However, in the ordinary FE-TM method, owing to round-off errors, they are not. The present SET method can offer solutions which can be strictly satisfied with the boundary conditions.

Table 6
Comparison of computation time for the shear-wall structure

Method by applying	Computation time (s)
FE	260
FE-TM	169
SET	124

Table 7
The maximum mode moment at the top boundary of the shear-wall structure (the maximum mode moment at all nodes is normalized to 1)

Mode numbers	SET	FE-TM
1	0.0	0.0002
2	0.0	0.0005
3	0.0	0.0023
4	0.0	0.0088
5	0.0	0.0213
6	0.0	0.0631
7	0.0	0.1026
8	0.0	0.1253
9	0.0	0.1548

4. Conclusions

In this paper, a stiffness equation transfer method has been proposed for obtaining natural frequencies of structures. Some numerical examples presented in this paper show that this method has the advantages of reducing the order of a matrix obtained by the FE method or the ordinary FE-TM method and minimizing the propagation of round-off errors occurring in recursive multiplications of transfer and point matrices. Furthermore, the drawback that the number of degrees of freedom on the left boundary must be the same as that on the right boundary in the ordinary FE-TM method, is avoided. It also has an additional advantage that in present method, one does not need to calculate so many values of the determinants and plot them versus assumed values of the frequencies. The present method, therefore, has potentially wider application than the ordinary FE-TM method.

Acknowledgements

The author would like to express his gratitude to Professor Fang and Dr Chen for their constructive suggestions.

Appendix A. Nomenclature

$U_i N_i$	displacement and internal force vectors of strip i, respectively
$U_i^L U_i^R$	displacement vectors on the left and right of section i, respectively
$N_i^L N_i^R$	internal force vectors on the left and right of section i, respectively
$U_{i+1}^L N_{i+1}^L$	displacement and internal force vectors on the left of section $i+1$, respectively
$[K]_i$	stiffness matrix of strip i
$[M]_i$	mass matrix of strip i
$[G]_i\ [K]_i - \omega^2[M]_i$	dynamic stiffness matrix of strip i
$[G_{11}]_i[G_{12}]_i[G_{21}]_i[G_{22}]_i$	sub-matrix of the matrix $[G]_i$
$[T]_i$	transfer matrix of strip i
$[P]\ [T]_n[T]_{n-1}\cdots[T]_1$	total transfer matrix of the structure
$[S]_i$	coefficient matrix of stiffness equation for section i
E_i	equivalent external force vectors on the section i
$[V]_i$	$[G_{11}]_i + [S]_i$
$[\dot{S}]_i$	derivative of $[S]_i$ with respect to frequency
$[Q]$	partitioned matrix
$[\dot{Q}]$	derivative of $[Q]$ with respect to frequency
$[Q_1][Q_2]\cdots,[Q_p]$	modified matrices of matrix $[Q]$
ω	frequency (rad/s)
E	Young's modulus
ρ	mass density
μ	the Poisson ratio

References

[1] M.A. Dokanish, A new approach for plate vibration: combination of transfer matrix and finite element technique, American Society of Mechanical Engineers, Journal of Engineering for Industry 94 (1972) 526–530.

[2] G. Chiatti, A. Sestieri, Analysis of static and dynamic structural problems by a combined finite element-transfer matrix, Journal of Sound and Vibration 67 (1) (1979) 35–42.

[3] M. Ohga, T. Shigematsu, T. Hara, A combined finite element-transfer matrix method: American Society of Civil Engineers, Journal of the Engineering Mechanics Division 110 (EM9) (1984) 1335–1349.

[4] E.E. Degen, M.S. Shephard, R.G. Loewy, Combined finite element-transfer matrix method based on a finite mixed formulation, Computers and Structures 26 (1985) 543–549.

[5] M. Ohga, T. Shiheematsu, Transient analysis of plates by a finite element-transfer matrix method, Computers and Structures 20 (1987) 173–180.

[6] Chen YuHua, Xue Huiyu, Dynamic large deflection analysis of structures by a combined finite element-Riccati transfer matrix method on a microcomputer, Computers and Structures 39 (6) (1991) 699–703.

[7] Xue Huiyu, A combined dynamic finite element-Riccati transfer matrix method for solving non-linear eigenproblems of vibrations, Computers and Structures 53 (1994) 1257–1261.

[8] Xue Huiyu, A combined finite element-Riccati transfer matrix method in frequency domain for transient structural response, Computers and Structures 62 (1997) 215–220.

[9] A. Jun-Yao Yu, Craggs, Transfer matrix method for finite element models of a chain-like structure under harmonic excitations, Journal of Sound and Vibration 187 (1) (1995) 169–175.

[10] N. Bhutani, R.G. Loewy, Combined finite element-transfer matrix method, Journal of Sound and Vibration 226 (5) (1999) 1048–1052.
[11] N. Feng, E.J. Hahn, A. Lattab, Further development of the combined FE-TM approach for evaluating the vibration behaviour of rotating machinery, International Conference on Computational Methods in Engineering, Singapore, 1992.
[12] M. Behzad, N. Feng, E.J. Hahn, Vibration analysis of rotor bearing systems using the Riccati transfer matrix method, International Mechanical Engineering Congress, Perth, Australia, 1994.
[13] A. Liew, N. Feng, E.J. Hahn, Application of transfer matrices to nonlinear rotor bearing systems, ASME Design Engineering Technical Conference: 17th Biennial Conference on Mechanical Vibration and Noise, Las Vegas, Nevada, 1999.
[14] A. Liew, N. Feng, E.J. Hahn, A nonlinear transfer matrix technique for statically indeterminate rotor bearing systems, International Mechanical Rotating Machines Conference, Nottingham, 2001.
[15] C. Horner, W.D. Pilkey, The Riccati transfer matrix method, ADAO 19848, 1975.
[16] P. Lancaster, Convergence of Newton–Raphson method of arbitrary polynomials, Mathematical Gazette 48 (1964) 291–295.
[17] P.N. Gustafson, W.F. Stokey, C.F. Zorowski, An experimental study of natural vibrations of cantilevered triangular plates, Journal of the Aeronautical Science 20 (1953) 331–337.
[18] J.L. Batoz, K.J. Bathe, L.W. Ho, A study of three-node triangular plate bending elements, International Journal for Numerical Methods in Engineering 15 (1980) 1771–1812.
[19] O.C. Zienkiewicz, The Finite Element Method, McGraw-Hill, New York, 1984.